IJARSCT
ISSN (Online) 2581-9429
International Journal of Advanced Research in Science, Communication and Technology (IJARSCT)
International Open-Access, Double-Blind, Peer-Reviewed, Refereed, Multidisciplinary Online Journal
Impact Factor: 7.53
Volume 4, Issue 3, March 2024

Thermal-Diffusion, Diffusion-Thermo Effects on MHD Mixed Convective Heat and Mass Transfer Inside Cone due to a Point Sink

Sayyed S. R [1] and Nasreen Bano [2]
Assistant Professor, Department of Mathematics, Doshi Vakil Arts and G.C.U.B. Science and Commerce College Goregaon, Raigad, M.S, India[1]
Assistant Professor, Department of Mathematics, G. M. Vedak College of Science, Tala, Raigad, M.S, India[2]
srsayyed786@gmail.com, snasreenbano@yahoo.in

Abstract*: The present investigation elucidates the magnetohydrodynamic (MHD) mixed convection phenomena involving heat and mass transfer within a cone influenced by a point sink, taking into account thermal diffusion and diffusion-thermo effects. Through the application of an appropriate similarity transformation, the boundary layer equations governing momentum, heat, and mass transfer were transformed into a set of ordinary differential equations. Subsequently, the obtained ordinary differential equations were addressed using the Homotopy Analysis Method (HAM) implemented through the BVPh 2.0 software package. The graphical representation and detailed discussion of dimensionless velocity, temperature, and concentration profiles were conducted to explore the influence of various governing parameters. Furthermore, the numerical results for the skin friction coefficient were compared with corresponding findings from the existing literature, revealing a notable agreement between them.*

Keywords: Magnetohydrodynamic, heat and mass transfer, mixed convection, Soret-Dufour effect, chemical reaction

I. INTRODUCTION

In recent decades, the analysis of heat and mass transfer in fluid flow influenced by a magnetic field has garnered substantial attention from researchers, owing to its diverse applications in geophysics, geothermal systems, technology, and engineering. The investigation of the boundary layer flow of an electrically conducting fluid directed towards the vertex of a cone, known as point sink flow, holds significance due to its practical relevance in nozzles or channels. This phenomenon was first examined by Choi and Wilhelm [1], and Rosenhead [2] made pioneering contributions to the understanding of fluid flow inside a cone due to a point sink in a classic text on laminar boundary layers. Ackerberg [3] provided a series solution for the converging motion of a viscous flow inside a cone, while Takhar et al. [4] extended the analysis to include an applied magnetic field, as well as heat and mass transfer. Eswara et al. [5] generalized the problem to unsteady scenarios by introducing transient motions in the free stream. Eswara and Bommaiah [6] explored the impact of variable viscosity on point sink flow. Magyari [7] investigated backward boundary layer flow with heat transfer in a converging channel, and Zhang et al. [8] further extended this analysis to magnetohydrodynamic (MHD) fluid flow. Fang and He [9] delved into the study of boundary layer flow due to a point sink inside a cone, considering mass transpiration and a moving wall condition. Guled and Singh [10] focused on the analysis of radiation effects on MHD flow with heat and mass transfer induced by a point sink.

The study of solutal and thermal transport, incorporating Soret and Dufour effects, finds applications in various fields including chemical reactions, colloidal science involving thermophoresis, and separation processes such as thermal diffusion and isotope separation. When a mixture experiences a temperature gradient, it triggers a phenomenon known as thermal diffusion or thermophoresis, which is closely associated with the Soret effect. Variations in the molecular mass and thermal diffusivities of solute species are the primary drivers of the Soret effect. The Dufour effect, also known as the 'mass diffusion thermal force,' arises from the interaction of concentration and temperature gradients within a mixture. Consequently, solute species migrate in response to changes in temperature and concentration.

IJARSCT
ISSN (Online) 2581-9429
International Journal of Advanced Research in Science, Communication and Technology (IJARSCT)
International Open-Access, Double-Blind, Peer-Reviewed, Refereed, Multidisciplinary Online Journal
Impact Factor: 7.53
Volume 4, Issue 3, March 2024

Researchers such as Pal et al. [11] have conducted studies on the mass and thermal transport of micro-polar fluids flowing over porous surfaces with variable thermal conduction, considering Soret and Dufour thermo effects. Yesodha et al. [12] examined the combined effects of Dufour and Soret, along with convective solutal and thermal transport of reacting fluids. Zhao et al. [13] investigated magnetohydrodynamic convective Maxwell fluid flow, incorporating solutal and thermal transport on porous surfaces with Soret and Dufour effects. Salahuddin et al. [14] analyzed the influence of Soret and Dufour effects on permeability flow in Carreau fluid flowing over a thermally radiated cylinder. Ketchate et al. [15] revealed instability accompanying magnetohydrodynamic convection of nanofluids in porous channels, considering the impacts of Dufour and Soret effects. Seid et al. [16] modeled nanofluid flow along vertical stretched surfaces, incorporating Soret and Dufour effects along with magnetic fields. Li et al. [17] investigated the framework of nanofluid flow with Darcy-Forchheimer flow towards stretched surfaces, considering the existence of Soret and Dufour effects. Ramudu et al. [18] explored the effects of MHD Casson fluid flowing across convective sheets, taking into account radiation, chemical reaction, and cross-diffusion phenomena.

The objective of this research paper is to conduct an analysis of magnetohydrodynamic (MHD) mixed convection heat and mass transfer within a cone, induced by a point sink and incorporating thermal diffusion, diffusion-thermo, and chemical reaction effects. The Homotopy Analysis Method (HAM) is employed for the resolution of the nonlinear ordinary differential equations (ODEs) governing the aforementioned problem. The solution process involves utilizing the Mathematica package BVPh 2.0 [19], designed for solving nonlinear boundary-value or eigenvalue problems characterized by boundary conditions at multiple points and governed by nonlinear ODEs. BVPh 2.0 is grounded in the HAM [20,21], which stands out as an analytical approximation method adept at addressing highly nonlinear problems. In contrast to perturbation techniques, the HAM is not contingent upon small/large physical parameters, positioning it as a non-perturbation method. Moreover, leveraging homotopy in topology, the HAM offers significant flexibility in selecting auxiliary linear operators and initial guesses. Importantly, the HAM uniquely provides a convenient mechanism for controlling and adjusting the convergence of solution series, ensuring the convergence of the solution series. The BVPh 2.0 Mathematica package, being HAM-based, serves as a user-friendly tool for solving nonlinear boundary-value or eigenvalue problems associated with coupled nonlinear ODEs. BVPh 2.0 is freely accessible online (http://numericaltank.sjtu.edu.cn/BVPh.htm).

II. PROBLEM DISCUSSION AND MATHEMATICAL FORMULATION

Consider a scenario involving a steady, laminar, axisymmetric flow of an electrically conducting incompressible fluid within a stationary circular cone, featuring a hole at the vertex. The boundary layer flow is induced by the presence of the hole, treated as a three-dimensional point sink. In this fluid dynamics process, we assume a very small magnetic Reynolds number, rendering the effects of the induced magnetic field negligible in comparison to the applied magnetic field. A magnetic field, denoted as B_0, is applied in the z-direction and is fixed relative to the fluid. Additionally, it is assumed that the injected fluid and the boundary layer fluid share identical physical properties. Constant values are attributed to the wall temperature (T_w) and concentration (C_w), as well as the ambient temperature (T_∞) and concentration (C_∞).

Under the aforementioned assumptions, the governing boundary layer equations governing the fluid flow, heat transfer, and mass transfer in the presence of thermal-diffusion and diffusion thermo effects can be expressed in cylindrical coordinates as:

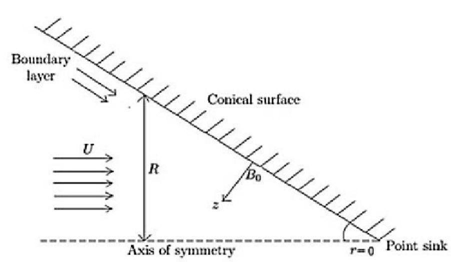

Fig. 1 The physical model and the coordinate system

IJARSCT

ISSN (Online) 2581-9429

International Journal of Advanced Research in Science, Communication and Technology (IJARSCT)

International Open-Access, Double-Blind, Peer-Reviewed, Refereed, Multidisciplinary Online Journal

Impact Factor: 7.53

Volume 4, Issue 3, March 2024

$$\frac{\partial u}{\partial r} + \frac{u}{r} + \frac{\partial w}{\partial z} = 0 \tag{1}$$

$$u\frac{\partial u}{\partial r} + w\frac{\partial u}{\partial z} = \nu\frac{\partial^2 u}{\partial z^2} - \sigma\frac{B_0^2}{\rho}u - \frac{1}{\rho}\frac{\partial p}{\partial r} + g\beta_t(T - T_\infty) + g\beta_C(C - C_\infty) \tag{2}$$

$$u\frac{\partial T}{\partial r} + w\frac{\partial T}{\partial z} = \alpha\frac{\partial^2 T}{\partial z^2} + \frac{\rho D_m K_t}{C_S C_p^2}\frac{\partial^2 C}{\partial z^2} \tag{3}$$

$$u\frac{\partial C}{\partial r} + w\frac{\partial C}{\partial z} = D\frac{\partial^2 C}{\partial z^2} + \frac{D_m K_t}{T_m}\frac{\partial^2 T}{\partial y^2} - K^*(C - C_\infty) \tag{4}$$

where $$-\frac{1}{\rho}\frac{\partial p}{\partial r} = U\frac{\partial U}{\partial r} + \sigma\frac{B_0^2}{\rho}U, \qquad U = -\frac{m_1}{r^2}, \quad m_1 > 0 \tag{5}$$

Here u and w are the velocity components along the r and z directions, respectively, B_0 is a constant applied magnetic field in z direction, ρ is fluid density, σ is the electrical conductivity, T is the fluid temperature, C is the fluid concentration, p represents the static pressure, $\alpha = \frac{k_1}{\rho C_p}$ is the thermal diffusivity, k_1 is thermal conductivity; D is the binary diffusion coefficient, ν is the kinematic viscosity, Cp is the specific heat at constant pressure, and m_1 is the strength of point sink., β_t is the coefficient of thermal expansion, β_C is the coefficient of solutal expansion, g is the gravitational constant, D_m is the mass diffusivity, K_T is the coefficient of thermal conductivity, C_S is the concentration susceptibility, T_m is the mean fluid temperature, K_f is the thermal diffusion ratio, K^* is the rate of chemical reaction, The appropriate boundary conditions by assuming slip effects are given by

$$\begin{gathered} u(r,0) = 0,\ w(r,0) = -V_w, T(r,0) = T_w,\ C(r,0) = C_w, \\ u(r,\infty) = U,\ \ T(r.\infty) = T_\infty,\ \ C(r,\infty) = C_\infty. \end{gathered} \tag{6}$$

where U is the inviscid flow velocity, $V_w < 0$ is the injection velocity, $V_w > 0$ gives the suction velocity.

We now introduce the similarity transformations

$$\eta = \frac{m_1^{\frac{1}{2}}z}{(2\nu r^2)^{\frac{1}{2}}},\ \ \psi(r,z) = -(2\nu m_1 r)^{\frac{1}{2}}f(\eta),\ \theta(\eta) = \frac{T - T_\infty}{T_w - T_\infty},\ \phi(\eta) = \frac{C - C_\infty}{C_w - C_\infty} \tag{7}$$

where η is the dimensionless similarity variable, f is the dimensionless stream function, θ is the dimensionless temperature, ϕ is the dimensionless concentration, the subscripts w and ∞ denote conditions at the wall and free stream, respectively and $\psi(r,z)$ is the dimensional stream function defined as

$$u = \frac{1}{r}\frac{\partial\psi}{\partial z}, \qquad w = -\frac{1}{r}\frac{\partial\psi}{\partial r}$$

which gives $$u = Uf'(\eta), \qquad w = \left(\frac{m_1\nu}{2r^3}\right)^{\frac{1}{2}}\left(f(\eta) - 3\eta f'(\eta)\right). \tag{8}$$

Eq. (1) is identically satisfied on account of Eqs. (7) and (8), and Eqs. (2) to (4) are transformed to

$$f''' - ff'' + 4(1 - f'^2) + M(1 - f') + \lambda(\theta + N\phi) = 0 \tag{9}$$

$$\frac{1}{Pr}\theta'' - f\theta' + D_f\phi'' = 0 \tag{10}$$

$$\frac{1}{S_C}\phi'' - f\phi' + S_r\theta'' - K\phi = 0 \tag{11}$$

Also, the boundary conditions (6) get reduced to

$$f(0) = s, \quad f'(0) = 1, \quad \theta(0) = 1, \quad \phi(0) = 1 \qquad (12)$$
$$f'(\infty) = 1, \quad \theta(\infty) = 0, \quad \phi(\infty) = 0$$

where $M = \frac{2\sigma B_0^2 r^3}{m_1 \rho}$ is the local magnetic parameter; $\lambda = \frac{Gr_r}{Re_r^2}$ is the mixed convection parameter, where $Gr_r = \frac{2g\beta_c(T_w - T_\infty)r^3}{\nu^2}$ is the Grashof number and $Re_r = \frac{Ur}{\nu}$ is a Reynold number (It is worth mentioning here that $\lambda > 0$ $(T_w > T_\infty)$ refers to a heated cone (assisting flow), $\lambda < 0 (T_w < T_\infty)$for a cooled cone (opposing flow) and $\lambda > 0$ $(T_w > T_\infty)$ corresponds to the forced convection flow case), $N = \frac{\beta_C(C_w - C_\infty)}{\beta_t(T_w - T_\infty)}$ is the constant dimensionless concentration buoyancy parameter. The ratio of Grashof numbers N appearing in equation (9) is the non-dimensional parameter representing the ratio between the buoyancy force due to concentration difference and the buoyancy force due to temperature difference. N is zero for no buoyancy effect due to mass diffusion, infinite for no buoyancy effect due to thermal diffusion, and is unity for thermal and mass buoyancy forces of the same strength. It is also positive for the case in which combined buoyancy forces are driving or assisting the flow and negative when the buoyancy forces are opposing each other; $Pr = \frac{\nu}{\alpha}$ is the Prandtl number; $D_f = \frac{D_m K_t(C_w - C_\infty)}{C_s C_p (T_w - T_\infty)\nu}$ is the Dufour number, $S_C = \frac{\nu}{D}$ is the Schmidt number, $S_r = \frac{D_m K_t (T_w - T_\infty)}{T_m (C_w - C_\infty)\nu}$ is the Soret number, $K = \frac{2K^* r^3}{m}$ is the chemical reaction parameter. The mass diffusion equation (11) can be adjusted to represent a destructive chemical reaction (means endothermic, i.e., heat is absorbed) if $K > 0$ or a generative chemical reaction (means exothermic, i.e., heat is generated) if $K < 0$ and $s = V_w \left(\frac{2r^3}{m_1 \nu}\right)^{1/2}$ is the local mass transfer parameter, where $s < 0$ corresponds to suction and $s > 0$ corresponds to injection, and the primes denote derivative with respect to η,

III. ANALYTICAL SOLUTION BY HAM

In 2012, Liao [] introduced the Homotopy Analysis Method (HAM)-based software package BVPh 1.0, designed for solving nonlinear boundary-value and eigenvalue problems characterized by singularity, multi-point boundary conditions, and multiple solutions, all governed by a single ordinary differential equation (ODE). Subsequently, a more recent version, BVPh 2.0, was released by Zhao and Liao for addressing nonlinear ODEs. Utilizing the Mathematica package BVPh 2.0, the system of coupled nonlinear ODEs (Equations 9 - 11) subject to the specified boundary conditions (Equation 12) can be effectively solved within the framework of the HAM. For brevity, this discussion provides a concise overview of the essential aspects related to BVPh 2.0. Comprehensive details about the HAM and BVPh 2.0 can be found in Liao's work []. BVPh 2.0 is user-friendly, requiring the definition of the governing equations and boundary conditions. The user selects an auxiliary linear operator for each governing equation, specifies the equation-type of the corresponding high-order equations, and provides a suitable initial guess for each unknown function. BVPh 2.0 then automatically generates analytic approximations at the desired order. Notably, a convergence-control parameter is assigned to each governing equation to ensure series solution convergence. The optimal values for these parameters are determined by minimizing the residual squares of the governing equations (and, in some cases, the boundary conditions). The HAM, grounded in homotopy in topology, effectively transforms a nonlinear problem into an infinite series of linear sub-problems without necessitating the consideration of small or large physical parameters.
For the problem under consideration, we have

$$f(\eta) = f_0(\eta) + \sum_{m=1}^{\infty} f_m(\eta) \qquad (13)$$

$$\theta(\eta) = \theta_0(\eta) + \sum_{m=1}^{\infty} \theta_m(\eta) \qquad (14)$$

$$\phi(\eta) = \phi_0(\eta) + \sum_{m=1}^{\infty} \phi_m(\eta) \qquad (15)$$

where $f_m(\eta), \theta_m(\eta)$ and $\phi_m(\eta)$ are determined by the so-called high-order deformation equations governed by the chosen auxiliary linear operators. According to Eqs. (9) - (11) and the boundary conditions (12) at infinity, it is obvious that $f(\eta), \theta(\eta)$ and $\phi(\eta)$ should be in the forms:

$$f(\eta)=\sum_{m=0}^{\infty}\sum_{k=0}^{\infty}a_{m,k}\eta^{k}e^{-m\eta} \tag{16}$$

$$\theta(\eta)=\sum_{m=0}^{\infty}\sum_{k=0}^{\infty}b_{m,k}\eta^{k}e^{-m\eta} \tag{17}$$

$$\phi(\eta)=\sum_{m=0}^{\infty}\sum_{k=0}^{\infty}c_{m,k}\eta^{k}e^{-m\eta} \tag{18}$$

where $a_{m,k}$, $b_{m,k}$ and $c_{m,k}$ are coefficients to be determined by the BVPh 2.0. Equations (16)-(18) serve as the solution expressions, offering valuable insights into the selection of auxiliary linear operators, initial approximations, and auxiliary functions within the context of the Homotopy Analysis Method (HAM). These equations play a crucial role in guiding the choice of these components in the HAM methodology.

Within the HAM framework, there exists considerable flexibility in the selection of auxiliary linear operators. In alignment with the solution expressions mentioned earlier, the following auxiliary linear operators can be chosen:

$$L_1(f)=\frac{d^3f}{d\eta^3}+\frac{d^2f}{d\eta^2} \tag{19}$$

$$L_2(\theta)=\frac{d^2\theta}{d\eta^2}-\theta \tag{20}$$

$$L_3(\phi)=\frac{d^2\phi}{d\eta^2}-\phi \tag{21}$$

which have the following properties

$$L_1(c_1+c_2\eta+c_3e^{-\eta})=0\; L_2(c_4e^{\eta}+c_5e^{-\eta})=0\; L_3(c_6e^{\eta}+c_7e^{-\eta})=0\,\} \tag{22}$$

where c_1, c_2, c_3, c_4, c_5, c_6 and c_7 are arbitrary constants.

In the frame of the HAM, we also have great freedom to choose the initial approximations and the auxiliary functions. According to the above-mentioned solution expression (16) - (18) and the boundary conditions (12), we choose the following initial approximations:

$$f_0(\eta)=s+\eta+\ (e^{-\eta}-1), \tag{23}$$

$$\theta_0(\eta)=\ e^{-\eta}, \tag{24}$$

$$\phi_0(\eta)=\ e^{-\eta}, \tag{25}$$

and the auxiliary functions as

$$H_f(\eta)=e^{-\eta},\qquad H_\theta(\eta)=e^{-\eta},\qquad H_\phi(\eta)=e^{-\eta} \tag{26}$$

It is here to be noted that the initial approximations must satisfy the boundary conditions (12). These are enough for the BVPh 2.0. Using the auxiliary linear operators (19)-(21), the initial approximations (23)-(25) and the auxiliary functions (26), the analytic approximations of the system of nonlinear ODEs (9)-(11) with the boundary conditions (12) can be gained automatically by the BVPh 2.0.

It should be emphasized that $f(\eta),\theta(\eta)$ and $\phi(\eta)$ given by the BVPh 2.0 contain two unknown convergence-control parameters c_0^f, c_0^θ and c_0^ϕ which are used to guarantee the convergence of the series solutions. It should be noticed that the convergence-control parameters play very important role in the frame of the HAM. It is the so-called convergence-control parameter that differentiates the HAM from all the other analytic approximation methods.

To greatly decrease the CPU time, [] used here the so-called average residual error at the m^{th}- order of approximation, defined by

$$\mathcal{E}_m^f(c_0^f,c_0^\theta,c_0^\phi)=\frac{1}{N+1}\sum_{j=0}^{N}\left[N_1\left(\sum_{i=0}^{m}f_i,\sum_{i=0}^{m}\theta_i,\sum_{i=0}^{m}\phi_i\right)|_{\eta=j\delta\eta}\right]$$

$$\mathcal{E}_m^\theta(c_0^f,c_0^\theta,c_0^\phi)=\frac{1}{N+1}\sum_{j=0}^{N}\left[N_2\left(\sum_{i=0}^{m}f_i,\sum_{i=0}^{m}\theta_i,\sum_{i=0}^{m}\phi_i\right)|_{\eta=j\delta\eta}\right]$$

IJARSCT

ISSN (Online) 2581-9429

International Journal of Advanced Research in Science, Communication and Technology (IJARSCT)

International Open-Access, Double-Blind, Peer-Reviewed, Refereed, Multidisciplinary Online Journal

Impact Factor: 7.53

Volume 4, Issue 3, March 2024

$$\mathcal{E}_m^{\phi}(c_0^f, c_0^{\theta}, c_0^{\phi}) = \frac{1}{N+1}\sum_{j=0}^{N} \left[N_3\left(\sum_{i=0}^{m} f_i, \sum_{i=0}^{m} \theta_i, \sum_{i=0}^{m} \phi_i\right)\Big|_{\eta=j\delta\eta} \right]$$

for the original governing equations, respectively, where N is an integer and N_1, N_2, N_3 are nonlinear differential operators defined by Eqs. (9)-(11), as follows:

$$N_1(f,\theta,\phi) = \frac{\partial^3 f}{\partial\eta^3} - f\frac{\partial^2 f}{\partial\eta^2} + 4\left[1-\left(\frac{\partial f}{\partial\eta}\right)^2\right] + M\left[1-\frac{\partial f}{\partial\eta}\right] + \lambda[\theta + N\phi]\ N_2(f,\theta,\phi)$$
$$= \frac{1}{Pr}\frac{\partial^2\theta}{\partial\eta^2} - f\frac{\partial\theta}{\partial\eta} + D_f\frac{\partial^2\phi}{\partial\eta^2}\quad N_3(f,\theta,\phi) = \frac{1}{S_c}\frac{\partial^2\phi}{\partial\eta^2} - f\frac{\partial\phi}{\partial\eta} + S_r\frac{\partial^2\theta}{\partial\eta^2} - K\phi\ \}$$

The total error at the m^{th} −order of approximation is defined by

$$\mathcal{E}_m^{t}(c_0^f, c_0^{\theta}, c_0^{\phi}) = \mathcal{E}_m^{f}(c_0^f, c_0^{\theta}, c_0^{\phi}) + \mathcal{E}_m^{\theta}(c_0^f, c_0^{\theta}, c_0^{\phi}) + \mathcal{E}_m^{\phi}(c_0^f, c_0^{\theta}, c_0^{\phi})$$

It is here to be noted that all the boundary conditions are linear and are exactly satisfied. At the m^{th} −order of approximation, the optimal values of $c_0^f, c_0^{\theta}, c_0^{\phi}$ are determined by the minimum of the total error $\mathcal{E}_m^t$, which can be done simply using **"GetOptiVar"**, a command of the BVPh 2.0.

IV. RESULT AND DISCUSSION

With the help of BVPh 2.0, we solved the transformed equation (15) with boundary conditions (16). In Table 1, a comparison of wall shear stress $f''(0)$ is made with the results published by Bashir et al. [34] in which $f''(0)$ is found for $N = 0$ and for different values of m.

From Table 2, it is evident that the present values of $f'(0)$ and $f''(0)$ obtained by BVPh 2.0 for different values of m and N are in excellent agreement with corresponding values of $f'(0)$ and $f''(0)$ which were obtained by Bashir et al. [34] by using an implicit finite difference under MATLAB to solve the problem. From Table 2, it is also seen that velocity profile increases with increase in values of m and N. Also, it is observed that wall shear stress increases with m while it decreases with N.

The effects of the power law parameter m on the velocity profiles are shown in Fig.2 for $N = 1$ and in Fig.3 for $N = -1$. It is noticed that as m increases, the velocity increases. The Figs. 4 and 5 depict the effect of slip parameter N on the velocity profiles for $m = 0.5$. It is seen that velocity increases with an increase in N.

TABLE I: OPTIMAL CONVERGENCE-CONTROL PARAMETERS AT DIFFERENT ORDERS OF APPROXIMATION IN THE CASE OF $M = 2$, $\lambda = N = 0.2$, $Pr = 7$, $D_f = 0.3$, $Sc = 0.22$, $Sr = 0.2$, $K = 0.1$ AND $s = -0.5$

m(order of approximation)	h_f	h_θ	h_ϕ	$\mathcal{E}_m^t$
1	−0.133829	−0.540395	−0.43201	1.84604×10^{-2}
3	−0.175356	−0.654194	−0.48913	3.13059×10^{-3}
6	−0.198367	−0.73158	−0.4905	8.12084×10^{-4}

TABLE II: AVERAGED SQUARED RESIDUAL ERRORS USING $h_f = -0.198367, h_\theta = -0.73158$ AND $h_\phi = -0.4905$ WHERE $M = 2$, $\lambda = N = 0.2$, $Pr = 7$, $D_f = 0.3$, $Sc = 0.22$, $Sr = 0.2$, $K = 0.1$ AND $s = -0.5$

m(order of approximatio	10	2 0	3 0	40
$\mathcal{E}_m^f$	1.12917×10^{-4}	2.17521×10^{-5}	1.11802×10^{-5}	4.74592×10^{-6}
$\mathcal{E}_m^\theta$	1.43183×10^{-4}	5.30636×10^{-5}	2.4316×10^{-6}	1.00506×10^{-6}
$\mathcal{E}_m^\phi$	1.20031×10^{-5}	0.30636×10^{-5}	1.6351×10^{-6}	0.9021×10^{-6}
$\mathcal{E}_m^t$	2.561×10^{-4}	7.48157×10^{-5}	1.36118×10^{-5}	5.7598×10^{-6}

IJARSCT
ISSN (Online) 2581-9429
International Journal of Advanced Research in Science, Communication and Technology (IJARSCT)
International Open-Access, Double-Blind, Peer-Reviewed, Refereed, Multidisciplinary Online Journal
Impact Factor: 7.53
Volume 4, Issue 3, March 2024

TABLE III: COMPARISON OF THE VALUES OF SKIN FRICTION COEFFICIENT $(f''(0))$ BY BVPH 2.0 WITH TAKHAR ET AL.[4] FOR $\lambda = N = D_f = Sr = K = 0$

M	s	$Present$	$Takhar\ et\ al.$ [4]
0	0	2.2721	2.2728
	1	1.7861	1.7505
	2	1.4167	1.4121
0.5	0	2.3827	2.392
	1	1.9117	1.973
	2	1.5232	1.5529
1.0	0	2.4604	2.4552
	1	2.0158	2.0825
	2	1.6252	1.6345
0	−2	3.5211	3.5182
	−1	2.8517	2.8772
0.5	−2	3.6172	3.6162
	−1	2.9554	3.0231
1.0	−2	3.7098	3.7124
	−1	3.0542	3.1121

Utilizing the Mathematica BVPh 2.0 package, the analytical solution for the system of nonlinear ordinary differential equations (9-11) with boundary conditions (12) has been obtained employing the Homotopy Analysis Method (HAM). For illustrative purposes, we consider the case where $M = 2$, $\lambda = N = 0.2$, $Pr = 7, D_f = 0.3$, $S_C = 0.22, Sr = 0.2$, $K = 0.1$ and $s = -0.5$. The optimal convergence-control parameters are determined using the "**GetOptiVar**" command of BVPh 2.0, and the results up to the 6th approximation are presented in Table 1. The total error $\mathcal{E}_m^t$ is reduced to 8.12084×10^{-4} with the corresponding optimal convergence-control parameters $h_f = -0.198367, h_\theta = -0.73158$ and $h_\phi = -0.4905$. The convergence of the analytic solution is confirmed by the decrease in the residual error of each governing equation, as indicated in Table 2. Thus, a convergent analytic solution is obtained for the specified problem under the given conditions. Similarly, one can extend this approach to obtain convergent analytic approximations for different physical parameters using BVPh 2.0. Table 3 demonstrates the validation of BVPh 2.0 for a two-dimensional magnetohydrodynamic (MHD) stagnation-point flow. Specifically, local skin friction coefficients $f''(0)$ are compared for various values of the magnetic parameter and suction/blowing parameter, excluding mixed convection, thermal diffusion, thermo-diffusion, and chemical reaction. The obtained results are compared with those of Thakar et al. [4].

The influence of the Dufour number (D_f), representing the reciprocal of the diffusion-thermo effect, and the Soret number (S_r), representing the reciprocal of the thermal-diffusion effect, on thermal, and solutal boundary layer thicknesses is elucidated in Figs. 2-5. Notably, an increase in the Dufour number leads to increase thermal boundary layer thicknesses and coupled with a decrease in solutal boundary layer thickness. These trends can be ascribed to the concentration difference increase or temperature difference decrease associated with higher Dufour numbers. Conversely, an increase in the Soret number results in decreased solutal boundary layer thicknesses, accompanied by an increase in thermal boundary layer thickness. This behaviour is explained by a decrease in concentration difference or an increase in temperature difference associated with higher Soret numbers.

V. CONCLUDING REMARKS

This study addresses the influence of, thermal-diffusion and diffusion-thermo effects on MHD heat and mass transfer within a cone induced by a point sink. The governing partial differential equations characterizing the system are transformed into ordinary differential equations using similarity transformations. Analytical solutions are obtained through the application of the Homotopy Analysis Method, allowing for the computation of heat and mass transfer

IJARSCT
ISSN (Online) 2581-9429
International Journal of Advanced Research in Science, Communication and Technology (IJARSCT)
International Open-Access, Double-Blind, Peer-Reviewed, Refereed, Multidisciplinary Online Journal
Impact Factor: 7.53
Volume 4, Issue 3, March 2024

characteristics across varying values of Dufour number and Soret number. The obtained numerical results are compared with previously reported findings in the literature, demonstrating excellent agreement.

Key findings from this investigation include:

The thermal boundary thickness exhibits a decreasing trend with Soret number. Conversely, an opposite trend is observed for Dufour number.

Concentration decreases with Dufour number and increases with Soret number.

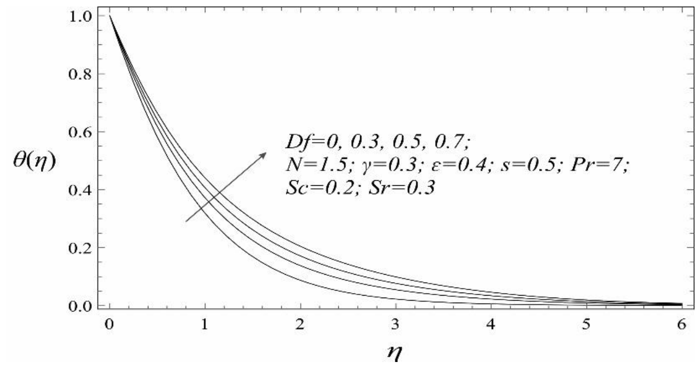

Fig. 2. Temperature profile for various values of D_f

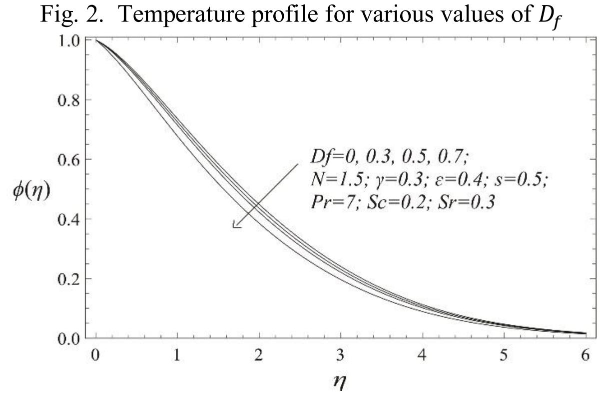

Fig. 3. Concentration profile for various values of D_f

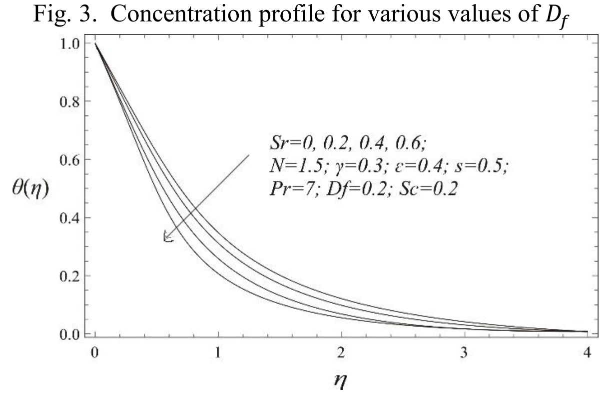

Fig. 4. Temperature profile for various values of S_r

IJARSCT
ISSN (Online) 2581-9429
International Journal of Advanced Research in Science, Communication and Technology (IJARSCT)
International Open-Access, Double-Blind, Peer-Reviewed, Refereed, Multidisciplinary Online Journal
Impact Factor: 7.53
Volume 4, Issue 3, March 2024

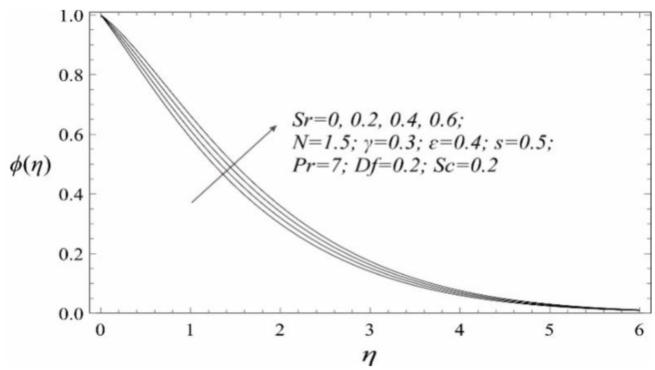

Fig. 5. Concentration profile for various values of S_r

REFERENCES

[1] S. H. Choi and H. E. Wilhelm, Self–similar magnetohydrodynamic diffuser flows with induced magnetic fields, Physics of Fluids, 20(11)(1977) 1821–1826..

[2] L. Rosenhead, Laminar Boundary Layers, Clarendon Press, Oxford, UK, 1963.

[3] R. C. Ackerberg, The viscous incompressible flow inside a cone, Journal of Fluid Mechanics, 21(1965) 47–81.

[4] H. S. Takhar, C. D. Surma Devi, and G. Nath, MHD flow with heat and mass transfer due to a point sink, Indian Journal of Pure and Applied Mathematics, 17(10) (1986) 1242–1247.

[5] A. T. Eswara, S. Roy, and G. Nath, Unsteady MHD forced flow due to a point sink, Acta Mechanica, 145(1-4)(2000) 159– 172.

[6] A. T. Eswara and B. C. Bommaiah, The effect of variable viscosity on laminar flow due to a point sink, Indian Journal of Pure and Applied Mathematics, 35(6)(2004) 811–815.

[7] E. Magyari, Backward boundary layer heat transfer in a converging channel." Fluid Dynamics Research 39(6)(2007) 493-504.

[8] J. Zhang, T. Fang, Y. Zhong, Analytical solution of magnetohyrodynamic sink flow. Appl. Math. Mech. 32(2011) 12-21.

[9] Fang and He, Boundary layer solutions to a point sink flow inside a cone with mass transpiration and moving wall, The European Physical Journal Plus, 130(21) (2015) (9 pages).

[10] C. N. Guled and B. B. Singh, Homotopy analysis of the radiation effect on MHD flow with heat and mass transfer due to a point sink, Advance in Mathematical Physics, 2016, 14 pages

[11] D. Pal, B.C. Das, K. Vajravelu, Magneto-Soret-Dufour thermo-radiative double diffusive convection heat and mass transfer of a micropolar fluid in a porous medium with Ohmic dissipation and variable thermal conductivity, Propulsion and Power Research 11 (1) (2022) 154–170.

[12] P. Yesodha, M. Bhuvaneswari, S. Sivasankaran, K. Saravanan, Convective heat and mass transfer of chemically reacting fluids with activation energy along with Soret and Dufour effects, Materials Today: Proceeding 42 (2021) 600–606.

[13] J. Zhao, L. Zheng, X. Zhang, F. Liu, Convection heat and mass transfer of fractional MHD Maxwell fluid in a porous medium with Soret and Dufour effects, International Journal of Heat and Mass Transfer 103 (2016) 203–210.

[14]] T. Salahuddin, A. Javed, M. Khan, M. Awais, H. Bangali, The impact of Soret and Dufour on permeable flow analysis of Carreau fluid near thermally radiated cylinder, International Communication of Heat and Mass Transfer 138 (2022) 106378.

[15] C.G.N. Ketchate, P.T. Kapen, D. Fokwa, G. Tchuen, Instability of MHD mixed convection flow of nanofluid in porous channel with thermal radiation, chemical reaction, Dufour and Soret effects, Chinese Journal of Physics (2023).

[16] E. Seid, E. Haile, T. alelign, Multiple slip, Soret and Dufour effects in fluid flow near a vertical stretching sheet in the presence of magnetic nanoparticles, International Journal of Thermofluids 13 (2022) 100-136.

[17] S. Li, M.I. Khan, M. Rafiq, S.A. Abdelmohsen, S.S. Abdullaev, M.S. Amjad, Optimized framework for Darcy-Forchheimer flow with chemical reaction in the presence of Soret and Dufour effects: a shooting technique, Chemical Physics Letters 825 (2023) 140578.
[18] A.C.V. Ramudu, K.A. Kumar, V. Sugunamma, N. Sandeep, Impact of Soret and Dufour on MHD Casson fluid flow past a stretching surface with convective–diffusive conditions, Journal of Thermal Analysis and Calorimetry (2022) 1–11.
[19] Y. Zhao, S. Liao, HAM-based package BVPh 2.0 for nonlinear boundary value problems, in: S. Liao (Ed.), Advances in Homotopy Analysis Method, World Scientific Press (2013).
[20] S. J. Liao, The proposed homotopy analysis technique for the solution of nonlinear prob lems, Ph.D. thesis, Shanghai Jiao Tong University, 1992.
[21] S.J. Liao, Beyond Perturbation: Introduction to Homotopy Analysis Method, Chapman and Hall/CRC Press, Boca Raton, 2003.
[22] S. J. Liao, Homotopy Analysis Method in Nonlinear Di erential Equations, Spring, Hei dilberg (2012).